



**University of  
Zurich<sup>UZH</sup>**

**Zurich Open Repository and  
Archive**

University of Zurich  
University Library  
Strickhofstrasse 39  
CH-8057 Zurich  
[www.zora.uzh.ch](http://www.zora.uzh.ch)

---

Year: 2014

---

## **Critical role of aquaporins in IL-1 -mediated inflammation**

Rabolli, Virginie ; Wallemme, Laurent ; Lo Re, Sandra ; Uwambayinema, Francine ; Palmai-Pallag, Mihaly ; Thomassen, Leen ; Tyteca, Donatienne ; Octave, Jean-Noel ; Marbaix, Etienne ; Lison, Dominique ; Devuyst, Olivier ; Huaux, François

**Abstract:** Rapid changes in cell volume characterize macrophage activation but the role of water channels in inflammation remains unclear. We show here that in vitro, AQP blockade or deficiency results in reduced IL-1 release by macrophages activated with a variety of NLRP3 stimuli. Inhibition of AQP specifically during the regulatory volume decrease process is sufficient to limit IL-1 release by macrophages through the NLRP3 inflammasome axis. The immune-related activity of AQP was confirmed in vivo in a model of acute lung inflammation induced by crystals. AQP1 deficiency is associated with a marked reduction of both lung IL-1 release and neutrophilic inflammation. We conclude that AQP-mediated water transport in macrophages constitutes a general danger signal required for NLRP3-related inflammation. Our findings reveal a new function of AQP in the inflammatory process and suggest a novel therapeutic target for anti-inflammatory therapy.

DOI: <https://doi.org/10.1074/jbc.M113.534594>

Posted at the Zurich Open Repository and Archive, University of Zurich

ZORA URL: <https://doi.org/10.5167/uzh-97246>

Journal Article

Accepted Version

Originally published at:

Rabolli, Virginie; Wallemme, Laurent; Lo Re, Sandra; Uwambayinema, Francine; Palmai-Pallag, Mihaly; Thomassen, Leen; Tyteca, Donatienne; Octave, Jean-Noel; Marbaix, Etienne; Lison, Dominique; Devuyst, Olivier; Huaux, François (2014). Critical role of aquaporins in IL-1 -mediated inflammation. *Journal of Biological Chemistry*, 289(20):13937-13947.

DOI: <https://doi.org/10.1074/jbc.M113.534594>

## Critical role of aquaporins in IL-1 $\beta$ -mediated inflammation

Virginie Rabolli<sup>1</sup>, Laurent Wallemme<sup>1</sup>, Sandra Lo Re<sup>1</sup>, Francine Uwambayinema<sup>1</sup>, Mihaly Palmai-Pallag<sup>1</sup>, Leen Thomassen<sup>2</sup>, Donatienne Tyteca<sup>3</sup>, Jean-Noel Octave<sup>4</sup>, Etienne Marbaix<sup>3</sup>, Dominique Lison<sup>1</sup>, Olivier Devuyst<sup>5</sup>, François Huaux<sup>1</sup>

<sup>1</sup>Louvain centre for Toxicology and Applied Pharmacology (LTAP), Institut de Recherche Experimentale et Clinique (IREC), Université catholique de Louvain, Brussels, Belgium.

<sup>2</sup>Center for Surface Chemistry & Catalysis, Katholieke Universiteit Leuven, Heverlee, Belgium.

<sup>3</sup>Cell Biology Unit, de Duve Institute, Université catholique de Louvain, Brussels, Belgium.

<sup>4</sup>Institute of NeuroScience (IoNS), Université catholique de Louvain, Brussels, Belgium.

<sup>5</sup>Institute of Physiology, Zurich Center for Integrative Human Physiology, University of Zurich, Zurich, Switzerland and Division of Nephrology, Institut de Recherche Experimentale et Clinique (IREC), Université catholique de Louvain, Brussels, Belgium.

Running title: *Aquaporins contribute to IL-1 $\beta$  activation.*

To whom correspondence should be addressed: François Huaux, Louvain centre for Toxicology and Applied Pharmacology (LTAP), Université catholique de Louvain, Avenue Mounier 53 bte B1.52.12, 1200 Brussels, Belgium. Phone: 00-32-2-764.53.39 - Fax: 00-32-2-764.53.38 - e-mail: francois.huaux@uclouvain.be

Keywords: Interleukin-1 $\beta$ , caspase, inflammation, aquaporin, water channel, inflammasome, cell swelling and RVD.

**Background:** Aquaporins are channels permeable to water and essential for immune cell migration.

**Results:** We demonstrate that aquaporin-mediated water fluxes are necessary for NLRP3 inflammasome-dependent release of mature IL-1 $\beta$  *in vitro* and *in vivo*.

**Conclusion:** Aquaporins are implicated in the mechanisms of pro-inflammatory cytokine secretion during inflammation.

**Significance:** The discovery of a new function for AQPs opens new diagnostic and therapeutic opportunities in inflammatory disorders.

### ABSTRACT

**Rapid changes in cell volume characterize macrophage activation but the role of water channels in inflammation remains unclear. We show here that *in vitro*, AQP blockade or deficiency results in reduced IL-1 $\beta$  release by**

**macrophages activated with a variety of NLRP3 stimuli. Inhibition of AQP specifically during the regulatory volume decrease process is sufficient to limit IL-1 $\beta$  release by macrophages through the NLRP3 inflammasome axis. The immune-related activity of AQP was confirmed *in vivo* in a model of acute lung inflammation induced by crystals. AQP1 deficiency is associated with a marked reduction of both lung IL-1 $\beta$  release and neutrophilic inflammation. We conclude that AQP-mediated water transport in macrophages constitutes a general danger signal required for NLRP3-related inflammation. Our findings reveal a new function of AQP in the inflammatory process and suggest a novel therapeutic target for anti-inflammatory therapy.**

Because of their ability to trigger or dampen inflammatory processes, macrophages are key effectors of innate immunity. They possess a wide range of specific receptors recognizing endogenous and foreign patterns indispensable to organize

adequate clearance and immune responses. Upon detection of threat signals, macrophages elicit immune reactions, trying to eliminate danger and to inform other cells by releasing cytokines and chemokines. In particular, the macrophage-derived cytokine IL-1 $\beta$  drives inflammation by enhancing granulocyte differentiation, migration and accumulation to inflammatory sites. This cytokine has been implicated in lung inflammatory reactions in response to bacteria, viruses, inorganic particles and drugs (1-4).

The release of mature IL-1 $\beta$  by macrophages requires the assembly of a multiproteic inflammasome complex of which the caspase-1 component is the final effector. The NLRP3 (NOD-like receptor protein 3) inflammasome is the most fully characterized inflammasome; it can be activated by a wide array of stimuli including extracellular adenosine triphosphate (ATP), bacterial toxins such as nigericin, monosodium urate crystals, environmental and industrial particles such as silica (5). How those structurally and chemically very different stimuli can activate this inflammasome in macrophages is still under investigation but common cellular stress signals are likely involved. It has been established that ionic movements represent a common event required for inflammasome activation by diverse stimuli. A drop in cytosolic K<sup>+</sup> is necessary and sufficient for caspase-1 activation and IL-1 $\beta$  release by macrophages (5). Cell distension and subsequent regulatory volume decrease (RVD) mediated by activation of volume sensor systems such as transient receptor potential (TRP) channels have also been associated to inflammasome activation in macrophages (6-8). However, the potential importance of channel-mediated water transport as a general pathway of inflammasome activation remains unknown.

Aquaporins (AQP) are a family of channels which facilitate water transport across cell membranes in response to osmotic gradients. Aquaporin-1 (AQP1), the archetype of all aquaporins, is selectively permeable to water and involved in rapid cellular water fluxes and cell volume regulations (9). While AQPs are primarily expressed in epithelial and endothelial cells, these channels are also expressed in erythrocytes and immune cells such as macrophages, dendritic cells

and thymocytes (10-15). AQP are implicated in the phagocytic functions, activation and migration of immune cells (10,12,14).

We explored here the involvement of AQPs in mature IL-1 $\beta$  release by macrophages. We show that AQP-related cell water transport triggered by diverse NLRP3 soluble and particulate activators is sensed as a danger signal by macrophages and that AQPs are implicated in NLRP3 inflammasome activation *in vitro* and *in vivo*.

## EXPERIMENTAL PROCEDURES

### *Animal model.*

Female C57BL/6 mice were obtained from Janvier (Le Genest-Saint-Isle, France). Wild type (AQP1 +/+) and knock-out (AQP1 -/-) mice (16) were obtained from A.S. Verkman (University of California, San Francisco, CA) and developed as a SPF colony at the UCL Medical School (Brussels). Studies were performed on gender-matched littermates aged 8-12 weeks. The animals were housed in positive pressure air-conditioned units (25°C, 50% relative humidity) on a 12-hr light/dark cycle and had access to standard diet and tap water *ad libitum*. A suspension of crystalline silica particles (DQ12; d<sub>50</sub> = 2.2 $\mu$ m, a gift from Dr. Ambruster, Essen, Germany) in sterile 0.9% saline (Braun Medical, Diegem, Belgium) was injected directly into the lung by pharyngeal aspiration at a dose of 2.5mg/mouse. To sterilize and inactivate any trace of endotoxins, particles were heated at 200°C for 2 h immediately before suspension and administration. Bleomycin (Aventis, Brussels, Belgium) was suspended in sterile 0.9% NaCl, and 1.25 U/kg body weight (b.wt.) was injected directly into the lung by pharyngeal aspiration. The experimental protocol was approved by the local ethical committee for animal research at the Université catholique de Louvain (2010/UCL/MD/034) and conformed to the Belgian and European Community regulations (LA1230312 and CEE n° 86/609).

### *Broncho-alveolar lavage (BAL) and alveolar neutrophil number.*

Mice were sacrificed after 6 hours with an intraperitoneal injection of sodium pentobarbital

(20 mg/mice) and bronchoalveolar lavage was performed by cannulating the trachea and lavaging the lung 4x with 1ml of NaCl 0.9%. The BAL fluid was centrifuged at 281g, 10 min, 4°C (Centrifuge 5804R, Eppendorf, Hamburg, Germany). Cells recovered in BAL were fixed in 1.25% paraformaldehyde and analyzed with FACS calibur (BD Biosciences) using FlowJo software. Neutrophils were identified by labelling with anti-GR1-PE (clone RB6-8C5, BD Biosciences, Erembodegem, Belgium) and their number calculated in function of total BAL cells counted with a Burker cell chamber. Fc receptors were blocked with anti-CD16/CD32 (clone 2.4G2, BD Biosciences) to reduce nonspecific binding.

### ***Lung histopathology.***

Lungs were lavaged and perfused with 0.9% NaCl and superior left lung lobe was fixed in 3.6% formaldehyde solution during one night; then paraffin-embedded 5- $\mu$ m sections were stained with hematoxylin and eosin. Images were acquired with a microscope Zeiss Jena Model Jenalumar equipped with an Apochromat 12,5x/0,35 for picture in large panel and a Planachromat fl 50x/0,95 for picture in the inserts (Carl Zeiss, Munich, Germany). The microscope was connected to Coolpix 4500 camera (Nikon, Kingston Upon Thames, UK).

### ***RNA extraction and quantification***

Total RNA extraction and quantification by qPCR were performed as described (17). Sequences of interest were amplified by PCR using the following forward primers (Invitrogen) : CGG CTA CCA CAT CCA AGC AA (mouse 18s RNA), GAC GGA CCC CAA AAG ATG AAG (mouse IL-1 $\beta$ ), CCA GCC AGA GTG GAA CTT TCG (mouse NLRP3), GGA GCT CAC AAT GAC TGT GCT TA (mouse ASC), GGA CTT CTC AAG ATC ATG GCT ACT T (mouse CXCR2), GAC TGC GAC TTC CTG GAG GAT (mouse ngp) and reverse primers: ATA CGC TAT TGG AGC TGG ATT ACC (mouse 18s RNA), CTC TTC GTT GAT GTG CTG CTG TG (mouse IL-1 $\beta$ ), TAC AAA TGG AGA TGC GGG AGA (mouse NLRP3), CTG CCA CAG CTC CAG ACT CTT(mouse ASC), TAG TAG AGG TGT TTG CTG AAG ACG A (mouse CXCR2), GTA TCC TCT CGA CTG CAA TCC CTG (mouse ngp).

### ***Enzyme-linked immunosorbent assays (ELISA)***

ELISA kits were used to measure IL-1 $\beta$  and IL-6 (R&D Systems, Wiesbaden-Nordenstadt, Germany). Assays were run according to the manufacturer's protocols with a detection limit of 15 pg/ml. The IL-1 $\beta$  assay selectively measure the mature form of IL-1 $\beta$  (17 kD) (18).

### ***Cell purification.***

Mice were sacrificed by intramuscular injection of 60 mg sodium pentobarbital. For peritoneal macrophages, the peritoneal cavity was lavaged with 10 ml of sterile NaCl 0.9% and centrifuged (280  $\times$  g, 10 min, 4°C). Macrophages were purified from peritoneal lavage based on their F4/80 expression by using magnetic cell separation (MACS; Miltenyi Biotec, Bergisch Gladbach, Germany) according to the manufacturer's protocol. For lung macrophages, lungs were perfused via the right heart ventricle with sterile NaCl 0.9% then 1 ml of enzyme mix containing 20 mg of pronase (Sigma-Aldrich, Bornem, Belgium) and 1mg of dnase (Worthington Biochemical Corporation, Lakewood, USA) in HBSS (Invitrogen; Merelbeke; Belgium) with 1 % of antibiotic antimycotic (AA) (fungizone (25  $\mu$ g/mL), penicillin–streptomycin (10000 U and 10000  $\mu$ g/mL; Invitrogen) were infused in cannulated trachea. After 20 minutes, lungs were excised and placed into a tube chilled on ice with fetal bovine serum (FBS) (Invitrogen). Collected lungs were then crushed by repeated aspiration and expulsion in a 20 ml syringe and passed on a 70  $\mu$ m filter. The filtered fraction was grown in 75cm<sup>2</sup> tissue culture flasks in DMEM (Invitrogen) supplemented with 10% FBS and 1 % of AA then detached using trypsin (Invitrogen). Lung macrophages were purified based on their CD45 expression by using magnetic cell separation (MACS; Miltenyi Biotec) according to the manufacturer's protocol. Macrophages were primed during 18 hours by exposure to 0.1  $\mu$ g/ml of purified LPS (Enzo Life Sciences, Antwerpen, Belgium) in complete medium.

### ***Inflammasome activation.***

LPS-primed cells (200,000 cells/well in 96-well plates, 7  $\times$  10<sup>6</sup> cells/well in 6 well plates) were exposed to an inflammasome activator (200  $\mu$ l)



during 30 minutes for ATP (5 mM), 1 hour for nigericin (Ng) (20  $\mu$ M), Stöber silica nanoparticles (SNP) (100  $\mu$ g/ml) and hypotonic shock, and 3 hours for DQ12 (400  $\mu$ g/ml). Supernatants and cell pellets were collected for mature IL-1 $\beta$  and active caspase-1 measurements. Stöber based synthesis process and characterization of SNP were described elsewhere (19). SNP diameter assessed by transmission electron microscopy or by dynamic light scattering in DMEM is 12.2 nm or 100 nm, respectively. Total surface area evaluated by BET (Brunauer, Emmet and Teller) model was of 400 m<sup>2</sup>/g. Isotonic and hypotonic media were prepared based on Perregaux (1996). Isotonic solution contains : 0.9 M CaCl<sub>2</sub>, 0.5 mM MgCl<sub>2</sub>, 1.5 mM KH<sub>2</sub>PO<sub>4</sub>, 2.7 mM KCl, 5 mM glucose, 20 mM Hepes and 137 mM NaCl. In hypotonic solutions, NaCl was absent (47 mosm/kg H<sub>2</sub>O) or at concentration reduced to 3.75 mM (53 mosm/kg H<sub>2</sub>O), 7.5 mM (60 mosm/kg H<sub>2</sub>O), 15 mM (66 mosm/kg H<sub>2</sub>O) or 30 mM (100 mosm/kg H<sub>2</sub>O). All solutions were prepared in LPS free water (Baxter, Braine-l'Alleud, Belgium) and filtered on 0.22  $\mu$ m filter. Hypertonic solutions were obtained by adding 100 mM NaCl (415 mosm/kg H<sub>2</sub>O) or 200 mM mannitol to DMEM. When a pretreatment was required, cells were first incubated with HgCl<sub>2</sub> 30 minutes prior to the activator; HgCl<sub>2</sub> was maintained in the medium till the end of the experiment. For mercurial AQP inhibition after hypotonic shock, HgCl<sub>2</sub> was added at different time points following hypotonic shock and maintained till the end of the experiment (60 min after the shock). For TRP inhibition, ruthenium red (Sigma-Aldrich) was added when hypotonic shock was applied and maintained till the end of the experiment (60 minutes after the shock). For cytotoxicity assay, cells were incubated in DMEM with 2 % WST1 (Roche Applied Science, Vilvoorde, Belgium) during 15 minutes.

#### ***Active caspase-1 measurement.***

After treatment with inflammasome activators, cells were incubated with green fluorescent peptide 5-carboxyfluorescein-Tyr-Val-Ala-Asp-fluoromethyl ketone, according to the manufacturer's recommendations (Immunochemistry Technologies, Bloomington, U.S.A.). Fluorescence was measured by using SPECTRAmax GEMINI XS Microplate

Spectrofluorometer (Molecular Devices, Sunnyvale, United States). For flow cytometry assay, 10<sup>6</sup> cells were exposed to hypotonic medium during 30 or 60 minutes in microtubes then incubated with the probe according to the manufacturer's recommendations and analysed by using a FACS Calibur (BD Biosciences, Erembodegem, Belgium).

#### ***Size modification assessment.***

For microscopical analysis of size modification, LPS-primed cells (300,000 cells/well in 48-well plates) were exposed to isotonic or hypotonic medium and pictures were taken after the required time of incubation in optimal culture condition. Images were acquired with the Zeiss AxioObserver.z1 equipped with a T° and pO<sub>2</sub>/pCO<sub>2</sub> regulation chamber and an EC "Plan-Neofluar" 10x/0.30 objective (Carl Zeiss). The microscope was connected to an AxioCam camera using AxioVision software (Carl Zeiss). For flow cytometry assessment of cell volume modification, LPS-primed cells were incubated in microtubes in isotonic or hypotonic medium during the desired time with or without mercury treatment. Cells were then fixed by addition of paraformaldehyde directly in the medium and analyzed with FACS calibur.

#### ***Western blot***

After treatments, supernatants of LPS-primed macrophages (7 10<sup>6</sup> cells/well in 6 well-plates) were collected and cell pellets were lysed on ice in Triton lysis buffer (TLB) (1% Triton, 25mM Tris pH 7.4, 150mM NaCl and 2 mg/ml anti-protease tablets, Roche Applied Science). Supernatant were concentrated by methanol – chloroform precipitation then suspended in 30  $\mu$ l of Laemmli buffer (Biorad, Nazareth Eke, Belgium). Supernatant and cell samples were sonicated 5 minutes in a bath (Bransonic-12, Geneva, Switzerland), heated at 99° C for 5 minutes and centrifuged 10 minutes at 14.000 rpm. Samples were loaded onto a 4-20% polyacrylamide gel (Mini- PROTEAN TGX, Bio-Rad, Hercules, USA) and transferred on a PVDF membrane (Millipore) by electro-blotting. Membranes were incubated overnight at 4°C with primary antibody (0.2  $\mu$ g/ml, polyclonal goat anti-IL-1 $\beta$  antibody, AF-401-NA, R&D Systems; 2  $\mu$ g/ml, polyclonal rabbit anti-

caspase-1 p10 antibody, clone M-20, Santa Cruz Biotechnology, Santa Cruz, USA or 1  $\mu$ g/ml, monoclonal mouse anti- $\beta$ -actin antibody, A1978, Sigma-Aldrich). After washing, membranes were incubated 1 hour with R dye infrared secondary antibodies (1:15 000; donkey IgG anti-goat, donkey IgG anti-rabbit or donkey IgG anti-mouse; Westburg, Leusden, The Netherlands). Detection was performed with Odyssey CLx Western Blot Detection System (Westburg).

### Statistics

Results were analyzed by Student Newman-Keuls test. Statistical significance was considered at  $P < 0.05$ .

## RESULTS

### *AQP-facilitated water transport induces NLRP3 inflammasome-related IL-1 $\beta$ activation and release in macrophages.*

As macrophage swelling is commonly recorded following exposure to different NLRP3 inflammasome activators (8), we analyzed the importance of water transport in IL-1 $\beta$  release *in vitro*. We first contained cell swelling in ATP-activated lung macrophages by exposure to increased extracellular tonicity (20). Under extracellular hyperosmolar conditions, ATP-induced IL-1 $\beta$  release by LPS-primed lung macrophages was significantly reduced (Fig. 1 a). The absence of cytotoxicity due to increased extracellular osmolarity was verified by measuring cellular mitochondrial activity (Fig. 1 d). To determine whether this effect was specific to inflammasome activation, we also measured the levels of the pro-inflammatory cytokine IL-6 which does not directly require inflammasome activation for its secretion. Unlike IL-1 $\beta$ , the release of IL-6 was not modified by extracellular hyperosmolar conditions (Fig. 1 e), suggesting that swelling is not required for the release of other pro-inflammatory cytokines which do not directly depend on inflammasome for their release. The inhibitory effect of an extracellular hyperosmolarity on ATP-induced inflammasome activation was confirmed in peritoneal macrophages based on the same protocol (Fig. 1 b). IL-1 $\beta$  release by peritoneal macrophages was also reduced when osmolarity was increased by

mannitol addition (Fig. 1 c). These results showed that rapid cell swelling is necessary for IL-1 $\beta$  release in macrophages.

To study water channel implication, a model of osmotic swelling-induced NLRP3 inflammasome activation and IL-1 $\beta$  release was used (7). IL-1 $\beta$  release was assessed in lung macrophages exposed during 60 minutes to hypotonic solutions with decreasing osmolarity. Reducing medium osmolarity to 100 and 66 mosm/kg H<sub>2</sub>O had no significant impact on IL-1 $\beta$  detected in cell supernatant but more drastic hypotonic conditions (from 60 to 47 mosm/kg H<sub>2</sub>O) progressively induced significant IL-1 $\beta$  release (Fig. 2 a). To test the involvement of water channels in that process, we treated cells 30 minutes before the hypotonic shock with mercury which pharmacologically inhibits most AQPs by interacting with an extracellular cysteine residue (21). The implication of AQPs in osmotic swelling was studied 2 minutes after exposure of lung macrophages to 60 mosm/kg H<sub>2</sub>O. At this time point, the size of cells exposed to hypotonic medium was increased compared to isotonic medium. This swelling was reduced in mercury treated cells (Fig. 2 b). AQP inhibition decreased the release of IL-1 $\beta$  by lung macrophages submitted to hypotonic shock (Fig. 2 c). We also explored the response of peritoneal macrophages treated according the same protocol. The reduction of IL-1 $\beta$  release was confirmed when AQPs were inhibited in peritoneal macrophages submitted to hypotonic shock (Fig. 2 d). This effect was supported by western blot data (Fig. 2 e). The release of mature IL-1 $\beta$  (IL-1 $\beta$  p17) by peritoneal macrophages in response to hypotonic shock was reduced upon mercury exposure. The decrease of intracellular pool of IL-1 $\beta$  pro-form (IL-1 $\beta$  p37) consecutive to hypotonic shock was moderated by AQP blockade (Fig. 2 e). Mercurial AQP inhibition also resulted in reduced caspase-1 activation consecutive to hypotonic shock in lung macrophages (Fig. 2 f). Together, these results demonstrated that rapid cell swelling via AQPs leads to NLRP3 inflammasome-related release of mature IL-1 $\beta$  by macrophages.

The requirement of AQPs was extended to other soluble and insoluble NLRP3 inflammasome activators. The concentration of IL-1 $\beta$  detected in the supernatant of lung macrophages after silica (DQ12) and ATP was significantly lower when

AQPs were inhibited (Fig. 2 g and i). Similarly, mercury inhibition of AQP led to decreased silica- (Fig. 2 h) and ATP- (Fig. 2 j) induced IL-1 $\beta$  release in peritoneal macrophages. Implication of AQP in caspase-1 activation (active caspase-1, casp1 p10) and mature IL-1 $\beta$  release was confirmed by western blotting in ATP-treated peritoneal macrophages (Fig. 2 k). AQP blockade also decreased ATP-induced reduction of intracellular IL-1 $\beta$  proform. Absence of cytotoxicity (Fig. 2 l) and IL-6-release modifications (Fig. 2 m) in the presence of mercury was verified in lung macrophages exposed to ATP. Together, these data thus indicated that rapid water transport via AQPs leads to IL-1 $\beta$  activation and release by lung and peritoneal macrophages after exposure to soluble and particulate NLRP3 stimuli.

***AQP-facilitated RVD is sufficient to induce NLRP3 inflammasome-related release of mature IL-1 $\beta$  in macrophages.***

We next investigated which phase of the AQP-dependent volume changes - initial swelling or subsequent volume restoration - mediates inflammasome activation in macrophages. First, the kinetics of volume modifications, caspase-1 activation and IL-1 $\beta$  release after hypotonic shock in lung macrophages were monitored. Cell swelling was obvious 2 minutes after exposure to hypotonic medium and sustained until 10 minutes. Subsequent size reduction was already perceptible 20 minutes after hypotonic shock and return to initial size was achieved after 45 and 60 minutes (Fig. 3 a to c). IL-1 $\beta$  excretion was detected 30 minutes after hypotonic shock, when the cell regulatory volume decrease (RVD) process started (Fig. 3 c). Similarly, active caspase-1 content in macrophages was detected 30 minutes after hypotonic shock and increased up to 1 hour (Fig. 3 d). The implication of cell volume sensor TRPs in IL-1 $\beta$  excretion was assessed by using ruthenium red. TRP inhibition resulted in decreased IL-1 $\beta$  release by lung macrophages in response to hypotonic shock (Fig. 3 e). These observations suggested that IL-1 $\beta$  release by macrophages arise from the RVD process consecutive to the initial cell swelling.

To clarify the role of AQPs in the RVD-related shrinkage process, HgCl<sub>2</sub> was added after cell

swelling (i.e. at 10, 20, 30, 40 or 50 minutes) upon hypotonic stress. Inhibition of AQPs after cell swelling and when RVD was initiated was sufficient to reduce mature IL-1 $\beta$  release (Fig. 3 f and g) without affecting intracellular IL-1 $\beta$  proform pool. This effect was not related to mercurial cytotoxicity (data not shown) nor IL-6 release modifications (Fig. 3 h). To confirm the inhibitory effect of mercury on RVD, cell size was assessed one hour after the shock when AQPs were inhibited 10 minutes after the shock (Fig. 3 i). These data indicated that volume restoration following cell swelling is implicated in NLRP3 inflammasome-related IL-1 $\beta$  release and that this process involves AQPs.

***AQP1 mediates NLRP3-related caspase-1 activation and mature IL-1 $\beta$  release in macrophages.***

We further investigated the implication of AQPs in NLRP3 inflammasome activation by targeting AQP1, a water specific channel expressed by immune cells (11,12,15). Cell swelling consecutive to hypotonic shock was reduced in AQP1 deficient cells (Fig. 4 a). AQP1 deficiency also reduced the release of mature IL-1 $\beta$  by lung (Fig. 4 b and c) and peritoneal (Fig. 4 d) macrophages submitted to hypotonic shock. Similarly, caspase-1 activation due to hypotonic shock was impaired in AQP1-deficient lung macrophages (Fig. 4 e). These results demonstrated that AQP1 leads to a rapid cell volume modification necessary for NLRP3 inflammasome activation and IL-1 $\beta$  release in response to osmotic shock.

Implication of AQP1 in NLRP3 inflammasome activation was extended to soluble and non-soluble inflammasome activators. AQP1 deletion decreased mature IL-1 $\beta$  release and caspase-1 activation by lung macrophages exposed to ATP (Fig. 4 f and g). The concentration of IL-1 $\beta$  detected in the supernatant of AQP1-deficient lung macrophages after nigericin, silica and silica nanoparticles (SNP) was also significantly lower in comparison to cells from WT mice (Fig. 4 h to j). We then verified whether AQP1 deletion could affect the expression of NLRP3 inflammasome components (Fig. 4 k to n). AQP1 deficiency did not modify the pool of IL-1 $\beta$  proform after LPS stimulation (Fig. 4 k and l). Similarly, no decrease in the expression of the pro-caspase-1 (Fig. 4 k,

caspl p45), NLRP3 (Fig. 4 m) or ASC (Fig. 4 n) was found in AQP1 deficient cells. These data thus indicated that AQP1 contributes to IL-1 $\beta$  activation and release by macrophages after exposure to NLRP3 soluble and particulate stimuli.

### ***AQP1 mediates crystal-induced NLRP3 inflammasome-dependent lung inflammation in mice.***

To verify whether aquaporin-mediated inflammasome activation has relevance in inflammation, we assessed the acute lung response of mice deficient in AQP1 to silica particles, a danger signal inducing NLRP3 inflammasome assembly and mature IL-1 $\beta$  release *in vivo* (22). Silica-induced lung inflammation is mainly characterized by an early accumulation of neutrophils and an increase of pro-inflammatory mediators both believed to be mediated by IL-1 $\beta$  (1,23). DQ12 was administered in the lung of AQP1  $+/+$  and  $-/-$  mice and acute lung inflammatory parameters were compared. Early neutrophilic inflammation was quantified by counting alveolar neutrophils and assessing the lung expression of specific markers such as neutrophilic granule protein (ngp) and CXCR2 (24). The cellular response to silica was evidenced by increased number of GR1 $^{+}$  cells in broncho-alveolar lavage (BAL) fluid (Fig. 5 a) and expression of neutrophilic markers in WT mice (Fig. 5 b and c), whereas lower levels of neutrophils as well as ngp and CXCR2 transcripts were detected in the lung of AQP1  $-/-$  mice. Silica-induced neutrophilic inflammation was also investigated histologically (Fig. 5 e to h). In hematoxylin and eosin-stained lung sections obtained from untreated mice, neutrophils were absent in WT and AQP1  $-/-$  samples (Fig. 5 e and f). When treated with silica, WT mice presented a more pronounced neutrophilic infiltration than AQP1 deficient mice (Fig. 5 g and h). Inflammasome activation was evaluated by the measurement of mature IL-1 $\beta$  in the alveolar space. The BAL fluid concentration of this cytokine was significantly increased after silica in WT mice and to a lower extent in AQP1 deficient animals (Fig. 5 d). In contrast to silica particles, lung inflammation induced by the antibiotic Bleomycin (not considered as direct NLRP3 activator) was not reduced in AQP1 deficient mice

(data not shown). In agreement with the *in vitro* observations, we concluded that AQP1 contributes to IL-1 $\beta$  release and neutrophilic inflammation in response to silica particles *in vivo*.

## **DISCUSSION**

Innate immune cells possess diverse sensors recognizing molecular patterns related to pathogenic or endogenous danger indicators, most sensors recognizing a limited number of patterns. Inflammasomes can activate caspase-1 in response to a great variety of stimuli including ATP, bacterial toxins, viral components, crystals and particles (2,15,20,22). The identification of a common element among these diverse stimuli that initiates inflammasome assembly may have a wide applicability in a range of inflammatory diseases (5).

Cell swelling is a hallmark of inflammatory conditions (25,26). In particular, swelling has been linked to macrophage activation and to its ability to induce inflammation by cytokine release (27-29). Interestingly, macrophage swelling and following RVD are recorded in association with NLRP3 inflammasome activation and IL-1 $\beta$  release in response to different stimuli (6-8,15,30). In the present study, we show the importance of AQP in cell volume changes, mainly RVD, for mature IL-1 $\beta$  release *in vitro* and *in vivo*. In particular, we demonstrated the implication of AQP1 in the development of neutrophilic inflammation. Rapid AQP-mediated water transport is thus sensed as a danger signal by the cell to trigger caspase-1 activation and mature IL-1 $\beta$  release in response to a variety of stimuli. The implication of AQPs in cell RVD and inflammasome activation is, however, not limited to AQP1. Mercury blocks most AQPs, thus its inhibitory effect on inflammasome activation could be related to different AQPs. Indeed, AQP9 is known to be expressed in leukocytes and activation of the mononuclear cells following intravenous endotoxin challenge results in modified expression of this water channel (13). Also, AQP9 inhibition has been linked to reduced inflammasome activation in response to monosodium urate crystals (15).

Several interactions of AQP with orchestrators of inflammasome activation can be proposed. Cells possess different volume sensor systems, such as



calcium permeable channel proteins TRP, driving RVD in macrophages. The activation of these channels and the associated ionic changes activate TAK1, a MAPKK kinase, necessary for hypotonicity-, alum-, ATP- and nigericin-induced mature IL-1 $\beta$  release and inflammation (7,8). In this study, we confirmed the implication of TRP in IL-1 $\beta$  release by macrophages in response to hypotonic shock. Interestingly, it has been observed that hypotonicity in salivary gland cells increased the association of TRPV4 and AQP5. In this case, TRP activation required AQP (31). RVD process implies an efflux of intracellular K<sup>+</sup> that has been shown necessary for inflammasome activation in response to various stimuli, including hypotonic shock (5,7,20). In this study, we found that intracellular potassium decrease was not reduced by AQP1 deficiency in lung macrophages exposed to hypotonic shock (data not shown). Thus the implication of AQP1 in IL-1 $\beta$  activation is not related to potassium efflux. Finally, it has been observed that inhibition of cell swelling and water flux by using mercury and phloretin reduced the capacity of macrophages to release mature IL-1 $\beta$  after monosodium urate crystals exposure (15). The authors concluded that water entry reduced intracellular potassium concentration to critical levels necessary for inflammasome assembly in this model. During the release process of mature IL-1 $\beta$ , active caspase-1/ASC aggregates abutted to external surface of actin filaments (32). Thus, it is also possible that AQP-mediated water efflux regulates caspase-1 processing and mature IL-1 $\beta$  release by modulating actin cytoskeletal rearrangements (33).

A possible implication of AQPs in inflammatory diseases has been proposed because of their role in cell migration and oedema formation (34). At the alveolar level, AQP1 and AQP5 are the most abundant with an endothelial or epithelial distribution, respectively (35,36). It has been shown that AQP5 knock-out mice develop less inflammation in a model of house dust mites-induced asthma (37). We observed that AQP1 deficiency reduces neutrophilic inflammation as well as cytokine release in silica-induced lung inflammation. Besides the respiratory tract, AQPs have been associated to inflammation in other organs (38,39). In a model of peritoneal dialysis,

reduced accumulation of leukocytes was observed in mice genetically deficient in AQP1 (40). AQP4 deficient mice developed less inflammation in a model of autoimmune encephalomyelitis (41). In light of our results, we propose that, in addition to their possible role in cell migration and oedema formation, AQP-mediated water fluxes in macrophages, subsequent RVD, and finally mature IL-1 $\beta$  release contribute to the inflammatory responses in these experimental models.

In humans, AQP alterations have also been correlated to several inflammatory diseases. Surexpression of AQP1 has been evidenced in auto-immune and alcoholic pancreatitis (42), in Alzheimer (43) as well as in rheumatoid and psoriatic arthritis cases (44). AQP4 expression is enhanced in the brain of Alzheimer disease and cerebral amyloid angiopathy suffering patients (43,45). AQP5 polymorphisms have been associated with COPD and chronic inflammation in smoking patients and survival rate in severe sepsis (46,47). These data further support a role of AQPs in human inflammatory diseases. Hemorrhagic shock and sepsis result in multiple organ failure, in particular acute lung injury, which may lead to death. IL-1 $\beta$  and NLRP3 activation have been implicated in this process (48,49). Interestingly, hypertonic solution has been shown to reduce inflammation and to increase the vital prognosis of these patients (50). The anti-inflammatory mechanism of this hypertonic resuscitation procedure is still unclear but, in light of our data, we postulate that it reduces AQP-mediated water transport and consecutively restricts inflammasome activation. Hence, AQPs should be considered as a new target in inflammation-associated disorders.

In conclusion, we demonstrated that rapid AQP-mediated cell swelling and mainly subsequent volume restoration are sensed as danger signals by macrophages and trigger NLRP3 inflammasome activation. AQP-mediated water movements appear as the common element unifying the variety of NLRP3 inflammasome activators. In vivo, AQPs contribute to inflammation by mediating mature IL-1 $\beta$  release.

## REFERENCES

1. Cassel, S. L., Eisenbarth, S. C., Iyer, S. S., Sadler, J. J., Colegio, O. R., Tephly, L. A., Carter, A. B., Rothman, P. B., Flavell, R. A., and Sutterwala, F. S. (2008) The Nalp3 inflammasome is essential for the development of silicosis. *Proceedings of the National Academy of Sciences of the United States of America* **105**, 9035-9040
2. Thomas, P. G., Dash, P., Aldridge, J. R., Jr., Ellebedy, A. H., Reynolds, C., Funk, A. J., Martin, W. J., Lamkanfi, M., Webby, R. J., Boyd, K. L., Doherty, P. C., and Kanneganti, T. D. (2009) The intracellular sensor NLRP3 mediates key innate and healing responses to influenza A virus via the regulation of caspase-1. *Immunity* **30**, 566-575
3. Hoshino, T., Okamoto, M., Sakazaki, Y., Kato, S., Young, H. A., and Aizawa, H. (2009) Role of proinflammatory cytokines IL-18 and IL-1 $\beta$  in bleomycin-induced lung injury in humans and mice. *American journal of respiratory cell and molecular biology* **41**, 661-670
4. Cai, S., Batra, S., Wakamatsu, N., Pacher, P., and Jeyaseelan, S. (2012) NLRC4 inflammasome-mediated production of IL-1 $\beta$  modulates mucosal immunity in the lung against gram-negative bacterial infection. *Journal of immunology* **188**, 5623-5635
5. Munoz-Planillo, R., Kuffa, P., Martinez-Colon, G., Smith, B. L., Rajendiran, T. M., and Nunez, G. (2013) K(+) Efflux Is the Common Trigger of NLRP3 Inflammasome Activation by Bacterial Toxins and Particulate Matter. *Immunity* **38**, 1142-1153
6. Perregaux, D. G., Laliberte, R. E., and Gabel, C. A. (1996) Human monocyte interleukin-1 $\beta$  posttranslational processing. Evidence of a volume-regulated response. *The Journal of biological chemistry* **271**, 29830-29838
7. Compan, V., Baroja-Mazo, A., Lopez-Castejon, G., Gomez, A. I., Martinez, C. M., Angosto, D., Montero, M. T., Herranz, A. S., Bazan, E., Reimers, D., Mulero, V., and Pelegrin, P. (2012) Cell volume regulation modulates NLRP3 inflammasome activation. *Immunity* **37**, 487-500
8. Gross, O., Yazdi, A. S., Thomas, C. J., Masin, M., Heinz, L. X., Guarda, G., Quadroni, M., Drexler, S. K., and Tschopp, J. (2012) Inflammasome activators induce interleukin-1 $\alpha$  secretion via distinct pathways with differential requirement for the protease function of caspase-1. *Immunity* **36**, 388-400
9. Agre, P., Sasaki, S., and Chrispeels, M. J. (1993) Aquaporins: a family of water channel proteins. *The American journal of physiology* **265**, F461
10. de Baey, A., and Lanzavecchia, A. (2000) The role of aquaporins in dendritic cell macropinocytosis. *The Journal of experimental medicine* **191**, 743-748
11. Moon, C., Rousseau, R., Soria, J. C., Hoque, M. O., Lee, J., Jang, S. J., Trink, B., Sidransky, D., and Mao, L. (2004) Aquaporin expression in human lymphocytes and dendritic cells. *American journal of hematology* **75**, 128-133
12. Jablonski, E. M., Webb, A. N., McConnell, N. A., Riley, M. C., and Hughes, F. M., Jr. (2004) Plasma membrane aquaporin activity can affect the rate of apoptosis but is inhibited after apoptotic volume decrease. *American journal of physiology. Cell physiology* **286**, C975-985
13. Talwar, S., Munson, P. J., Barb, J., Fiuza, C., Cintron, A. P., Logun, C., Tropea, M., Khan, S., Reda, D., Shelhamer, J. H., Danner, R. L., and Suffredini, A. F. (2006) Gene expression profiles of peripheral blood leukocytes after endotoxin challenge in humans. *Physiological genomics* **25**, 203-215
14. Zhu, N., Feng, X., He, C., Gao, H., Yang, L., Ma, Q., Guo, L., Qiao, Y., Yang, H., and Ma, T. (2011) Defective macrophage function in aquaporin-3 deficiency. *FASEB journal : official publication of the Federation of American Societies for Experimental Biology* **25**, 4233-4239
15. Schorn, C., Frey, B., Lauber, K., Janko, C., Stryio, M., Keppeler, H., Gaip, U. S., Voll, R. E., Springer, E., Munoz, L. E., Schett, G., and Herrmann, M. (2011) Sodium overload and water influx activate the NALP3 inflammasome. *The Journal of biological chemistry* **286**, 35-41
16. Ma, T., Yang, B., Gillespie, A., Carlson, E. J., Epstein, C. J., and Verkman, A. S. (1998) Severely impaired urinary concentrating ability in transgenic mice lacking aquaporin-1 water channels. *The Journal of biological chemistry* **273**, 4296-4299
17. Rabolli, V., Lo Re, S., Uwambayinema, F., Yakoub, Y., Lison, D., and Huaux, F. (2011) Lung fibrosis induced by crystalline silica particles is uncoupled from lung inflammation in NMRI mice. *Toxicology letters* **203**, 127-134

18. Herzyk, D. J., Berger, A. E., Allen, J. N., and Wewers, M. D. (1992) Sandwich ELISA formats designed to detect 17 kDa IL-1 beta significantly underestimate 35 kDa IL-1 beta. *Journal of immunological methods* **148**, 243-254
19. Thomassen, L. C., Aerts, A., Rabolli, V., Lison, D., Gonzalez, L., Kirsch-Volders, M., Napierska, D., Hoet, P. H., Kirschhock, C. E., and Martens, J. A. (2010) Synthesis and characterization of stable monodisperse silica nanoparticle sols for in vitro cytotoxicity testing. *Langmuir : the ACS journal of surfaces and colloids* **26**, 328-335
20. Perregaux, D., and Gabel, C. A. (1994) Interleukin-1 beta maturation and release in response to ATP and nigericin. Evidence that potassium depletion mediated by these agents is a necessary and common feature of their activity. *The Journal of biological chemistry* **269**, 15195-15203
21. Savage, D. F., and Stroud, R. M. (2007) Structural basis of aquaporin inhibition by mercury. *Journal of molecular biology* **368**, 607-617
22. Hornung, V., Bauernfeind, F., Halle, A., Samstad, E. O., Kono, H., Rock, K. L., Fitzgerald, K. A., and Latz, E. (2008) Silica crystals and aluminum salts activate the NALP3 inflammasome through phagosomal destabilization. *Nature immunology* **9**, 847-856
23. Dostert, C., Petrilli, V., Van Bruggen, R., Steele, C., Mossman, B. T., and Tschopp, J. (2008) Innate immune activation through Nalp3 inflammasome sensing of asbestos and silica. *Science* **320**, 674-677
24. Van Belle, A. B., de Heusch, M., Lemaire, M. M., Hendrickx, E., Warnier, G., Dunussi-Joannopoulos, K., Fouser, L. A., Renauld, J. C., and Dumoutier, L. (2012) IL-22 is required for imiquimod-induced psoriasiform skin inflammation in mice. *Journal of immunology* **188**, 462-469
25. Solez, K., Axelsen, R. A., Benediktsson, H., Burdick, J. F., Cohen, A. H., Colvin, R. B., Croker, B. P., Droz, D., Dunnill, M. S., Halloran, P. F., and et al. (1993) International standardization of criteria for the histologic diagnosis of renal allograft rejection: the Banff working classification of kidney transplant pathology. *Kidney international* **44**, 411-422
26. Bonventre, J. V., and Weinberg, J. M. (2003) Recent advances in the pathophysiology of ischemic acute renal failure. *Journal of the American Society of Nephrology : JASN* **14**, 2199-2210
27. Sokol, R. J., Hudson, G., James, N. T., Frost, I. J., and Wales, J. (1987) Human macrophage development: a morphometric study. *Journal of anatomy* **151**, 27-35
28. Pankow, W., Neumann, K., Ruschoff, J., and von Wichert, P. (1995) Human alveolar macrophages: comparison of cell size, autofluorescence, and HLA-DR antigen expression in smokers and nonsmokers. *Cancer detection and prevention* **19**, 268-273
29. Daigneault, M., Preston, J. A., Marriott, H. M., Whyte, M. K., and Dockrell, D. H. (2010) The identification of markers of macrophage differentiation in PMA-stimulated THP-1 cells and monocyte-derived macrophages. *PloS one* **5**, e8668
30. Palomaki, J., Valimaki, E., Sund, J., Vippola, M., Clausen, P. A., Jensen, K. A., Savolainen, K., Matikainen, S., and Alenius, H. (2011) Long, needle-like carbon nanotubes and asbestos activate the NLRP3 inflammasome through a similar mechanism. *ACS nano* **5**, 6861-6870
31. Liu, X., Bandyopadhyay, B. C., Nakamoto, T., Singh, B., Liedtke, W., Melvin, J. E., and Ambudkar, I. (2006) A role for AQP5 in activation of TRPV4 by hypotonicity: concerted involvement of AQP5 and TRPV4 in regulation of cell volume recovery. *The Journal of biological chemistry* **281**, 15485-15495
32. Pelegrin, P., and Surprenant, A. (2009) Dynamics of macrophage polarization reveal new mechanism to inhibit IL-1beta release through pyrophosphates. *The EMBO journal* **28**, 2114-2127
33. Papadopoulos, M. C., Saadoun, S., and Verkman, A. S. (2008) Aquaporins and cell migration. *Pflugers Archiv : European journal of physiology* **456**, 693-700
34. Verkman, A. S. (2012) Aquaporins in clinical medicine. *Annual review of medicine* **63**, 303-316
35. Towne, J. E., Harrod, K. S., Krane, C. M., and Menon, A. G. (2000) Decreased expression of aquaporin (AQP)1 and AQP5 in mouse lung after acute viral infection. *American journal of respiratory cell and molecular biology* **22**, 34-44
36. Jang, A. S., Lee, J. U., Choi, I. S., Park, K. O., Lee, J. H., Park, S. W., and Park, C. S. (2004) Expression of nitric oxide synthase, aquaporin 1 and aquaporin 5 in rat after bleomycin inhalation. *Intensive care medicine* **30**, 489-495
37. Shen, Y., Wang, Y., Chen, Z., Wang, D., Wang, X., Jin, M., and Bai, C. (2011) Role of aquaporin 5 in antigen-induced airway inflammation and mucous hyperproduction in mice. *Journal of cellular and molecular medicine* **15**, 1355-1363

38. Hardin, J. A., Wallace, L. E., Wong, J. F., O'Loughlin, E. V., Urbanski, S. J., Gall, D. G., MacNaughton, W. K., and Beck, P. L. (2004) Aquaporin expression is downregulated in a murine model of colitis and in patients with ulcerative colitis, Crohn's disease and infectious colitis. *Cell and tissue research* **318**, 313-323
39. Auguste, K. I., Jin, S., Uchida, K., Yan, D., Manley, G. T., Papadopoulos, M. C., and Verkman, A. S. (2007) Greatly impaired migration of implanted aquaporin-4-deficient astroglial cells in mouse brain toward a site of injury. *FASEB journal : official publication of the Federation of American Societies for Experimental Biology* **21**, 108-116
40. Nishino, T., and Devuyst, O. (2008) Clinical application of aquaporin research: aquaporin-1 in the peritoneal membrane. *Pflugers Archiv : European journal of physiology* **456**, 721-727
41. Li, L., Zhang, H., and Verkman, A. S. (2009) Greatly attenuated experimental autoimmune encephalomyelitis in aquaporin-4 knockout mice. *BMC neuroscience* **10**, 94
42. Ko, S. B., Mizuno, N., Yatabe, Y., Yoshikawa, T., Ishiguro, H., Yamamoto, A., Azuma, S., Naruse, S., Yamao, K., Muallem, S., and Goto, H. (2009) Aquaporin 1 water channel is overexpressed in the plasma membranes of pancreatic ducts in patients with autoimmune pancreatitis. *The journal of medical investigation : JMI* **56 Suppl**, 318-321
43. Huysseune, S., Kienlen-Campard, P., Hebert, S., Tasiaux, B., Leroy, K., Devuyst, O., Brion, J. P., De Strooper, B., and Octave, J. N. (2009) Epigenetic control of aquaporin 1 expression by the amyloid precursor protein. *FASEB journal : official publication of the Federation of American Societies for Experimental Biology* **23**, 4158-4167
44. Mobasheri, A., Moskaluk, C. A., Marples, D., and Shakibaei, M. (2010) Expression of aquaporin 1 (AQP1) in human synovitis. *Annals of anatomy = Anatomischer Anzeiger : official organ of the Anatomische Gesellschaft* **192**, 116-121
45. Moftakhar, P., Lynch, M. D., Pomakian, J. L., and Vinters, H. V. (2010) Aquaporin expression in the brains of patients with or without cerebral amyloid angiopathy. *Journal of neuropathology and experimental neurology* **69**, 1201-1209
46. Hansel, N. N., Sidhaye, V., Rafaeels, N. M., Gao, L., Gao, P., Williams, R., Connett, J. E., Beaty, T. H., Mathias, R. A., Wise, R. A., King, L. S., and Barnes, K. C. (2010) Aquaporin 5 polymorphisms and rate of lung function decline in chronic obstructive pulmonary disease. *PloS one* **5**, e14226
47. Adamzik, M., Frey, U. H., Mohlenkamp, S., Scherag, A., Waydhas, C., Marggraf, G., Dammann, M., Steinmann, J., Siffert, W., and Peters, J. (2011) Aquaporin 5 gene promoter--1364A/C polymorphism associated with 30-day survival in severe sepsis. *Anesthesiology* **114**, 912-917
48. Mao, K., Chen, S., Chen, M., Ma, Y., Wang, Y., Huang, B., He, Z., Zeng, Y., Hu, Y., Sun, S., Li, J., Wu, X., Wang, X., Strober, W., Chen, C., Meng, G., and Sun, B. (2013) Nitric oxide suppresses NLRP3 inflammasome activation and protects against LPS-induced septic shock. *Cell research* **23**, 201-212
49. Xu, P., Wen, Z., Shi, X., Li, Y., Fan, L., Xiang, M., Li, A., Scott, M. J., Xiao, G., Li, S., Billiar, T. R., Wilson, M. A., and Fan, J. (2013) Hemorrhagic shock augments Nlrp3 inflammasome activation in the lung through impaired pyrin induction. *Journal of immunology* **190**, 5247-5255
50. Oliveira, R. P., Velasco, I., Soriano, F. G., and Friedman, G. (2002) Clinical review: Hypertonic saline resuscitation in sepsis. *Critical care* **6**, 418-423



## FOOTNOTES

This work was funded by the Programme d'excellence « Marshall » Diane convention, by the Fonds de la Recherche Scientifique Médicale (FRSM), by Actions de Recherche Concertées, Communauté française de Belgique, Direction de la Recherche Scientifique (ARC 09/14-021), by the Fondation Contre le Cancer, by the Fonds de la Recherche Scientifique (FNRS ; Project PDR T.0119.13 14633768), by the European Commission under FP7-HEALTH-F4-2008 (Contract no. 202047) and by Agence Nationale de sécurité sanitaire de l'alimentation, de l'environnement et du travail (ANSES, France). They were supported in part by the Fondation Saint-Luc at UCL; a Baxter Extramural Grant; the Inter-University Attraction Pole (IUAP, Belgium Federal Government); the NCCR Kidney.CH program (Swiss National Science Foundation) and the Swiss National Science Foundation 310030-146490 (to OD).

F.H. is a Research Associate with the FNRS, Belgium.

The abbreviations used are : AQP, aquaporin; ASC, apoptosis-associated speck-like protein containing a CARD; BAL, broncho-alveolar lavage; DQ12, crystalline silica ( $\alpha$ -quartz); Ngp, neutrophilic granule protein; RVD, regulatory volume decrease; SNP, silica nanoparticles.

## FIGURE LEGENDS

### *Figure 1: Water entry is necessary for IL-1 $\beta$ release in macrophages.*

Release of IL-1 $\beta$  by (a) lung macrophages (LM) or (b) peritoneal macrophages (PM) primed with LPS (0.1  $\mu$ g/ml, overnight) and subsequently exposed or not to ATP (5 mM) with addition or not of NaCl to the medium (415 mosm/kg H<sub>2</sub>O). n=4 replicates per condition. (c) Release of mature IL-1 $\beta$  by peritoneal macrophages exposed or not to ATP (5 mM) with addition or not of mannitol to the medium (200 mM). n=3 or 4. (d) Mitochondrial activity assessed by optical density (OD) of reduced WST-1 and (e) release of IL-6 by lung macrophages exposed or not to ATP (5 mM) with addition or not of NaCl to the medium. n = 3 or 4. Values are means  $\pm$  SEM. \*\*\*p<0.001 denotes significant difference in values measured upon exposure to hypotonic ATP with or without NaCl or mannitol addition; ns, denotes no significant difference. P-values were calculated by the Student Newman-Keuls test.

### *Figure 2: AQP-facilitated water transport induces NLRP3 inflammasome-related caspase-1 activation and mature IL-1 $\beta$ release.*

(a) IL-1 $\beta$  release by lung macrophages (LM) primed with LPS (0.1  $\mu$ g/ml) exposed to isotonic (320 mosm/kg H<sub>2</sub>O) or hypotonic medium (100 mosm/kg H<sub>2</sub>O to 47 mosm/kg H<sub>2</sub>O). n=3 replicates per condition. (b) Flow-cytometry forward scatter plots of lung macrophages subjected or not to hypotonic shock (60 mosm/kg H<sub>2</sub>O) in absence or presence of HgCl<sub>2</sub> (10  $\mu$ M). Values indicated in plots are differences between median forward scatter of cells exposed or not to hypotonic shock. Levels of released IL-1 $\beta$  by (c) lung or (d) peritoneal macrophages (PM) exposed or not to hypotonic shock (in absence or presence of HgCl<sub>2</sub> (10  $\mu$ M). n = 3. (e) Western blot analysis of mature IL-1 $\beta$  (IL-1 $\beta$  p17) in the supernatant (SN) and pro-IL-1 $\beta$  (IL-1 $\beta$  p37) in cell lysate of peritoneal macrophages exposed or not to hypotonic shock in absence or presence of HgCl<sub>2</sub>. (f) Fluorimetric measurement of cellular active caspase-1 in lung macrophages exposed or not to hypotonic shock in absence or presence of HgCl<sub>2</sub> (10  $\mu$ M). n = 3 or 4. Release of IL-1 $\beta$  by (g) lung or (h) peritoneal macrophages exposed or not to silica (400  $\mu$ g/ml) in absence or presence of HgCl<sub>2</sub> (10  $\mu$ M). n = 3 or 4. IL-1 $\beta$  release by (i) lung or (j) peritoneal macrophages exposed or not to ATP (5 mM) in absence or presence of HgCl<sub>2</sub>. n = 3 or 4. (k) Western blot analysis of mature IL-1 $\beta$  (IL-1 $\beta$  p17) and active caspase-1 (Casp1 p10) in the supernatant and pro-IL-1 $\beta$  (IL-1 $\beta$  p37) in cell lysate of peritoneal macrophages exposed or not to ATP in absence or presence of HgCl<sub>2</sub>. (l) Mitochondrial activity assessed by optical density (OD) of reduced WST-1 and (m) release of IL-6 by lung macrophages exposed or not to ATP (5 mM) in absence or presence of HgCl<sub>2</sub> (10  $\mu$ M). n = 3 or 4.

Values are means  $\pm$  SEM. \*\* $p < 0.01$  and \*\*\* $p < 0.001$  denotes significant difference in values measured upon exposure to hypotonic medium or ATP or not, with HgCl<sub>2</sub> or not; ns, denotes no significant difference. P-values were calculated by the Student Newman–Keuls test.

**Figure 3: AQP1 mediates IL-1 $\beta$  activation during the cell volume reduction process in macrophages.**

(a) Optical microscopy (bar size, 4  $\mu$ m) and (b) flow-cytometry forward scatter plots of lung macrophages primed with LPS (0.1  $\mu$ g/ml) at different time points after hypotonic shock (60 mosm/kg H<sub>2</sub>O). Values indicated in the flow-cytometry plots are differences between median forward scatter (FSC) of cells exposed or not to hypotonic shock. (c) IL-1 $\beta$  release (left Y axis) and flow cytometry forward scatter (right Y axis) of lung macrophages at different time points after hypotonic shock. n=4 replicates per condition. (d) Flow-cytometry plot of intracellular active caspase-1 content in lung macrophages 30 or 60 minutes after hypotonic shock. IL-1 $\beta$  release by lung macrophages 1 h after hypotonic shock in the absence or presence of (e) ruthenium red (RR, 30  $\mu$ M) or (f) HgCl<sub>2</sub> (10  $\mu$ M, added 10, 20, 30, 40 or 50 minutes after hypotonic shock). n = 3 or 4. (g) Western blot analysis of mature IL-1 $\beta$  (IL-1 $\beta$  p17) in the supernatant (SN) and pro-IL-1 $\beta$  (IL-1 $\beta$  p37) in cell lysate of lung macrophages exposed or not to hypotonic shock in absence or presence of HgCl<sub>2</sub> (10  $\mu$ M, added 10, 20, or 50 minutes after hypotonic shock). (h) IL-6 release by lung macrophages 1 h after hypotonic shock in the absence or presence of HgCl<sub>2</sub> (10  $\mu$ M, added 10, 20, 30, 40 or 50 minutes after hypotonic shock). n = 3 or 4. (i) Flow-cytometry forward scatter plots of lung macrophages 1 h after hypotonic shock in presence or absence of HgCl<sub>2</sub> (10  $\mu$ M, added 10 minutes after hypotonic shock). Values indicated in the plots are differences between median forward scatter of cells exposed or not to hypotonic shock. Values are means  $\pm$  SEM. \* $p < 0.05$  and \*\*\* $p < 0.001$  denote significant difference in values measured upon exposure to hypotonic medium with ruthenium red or HgCl<sub>2</sub> or not; ns, denotes no significant difference. P-values were calculated by a Student Newman–Keuls test.

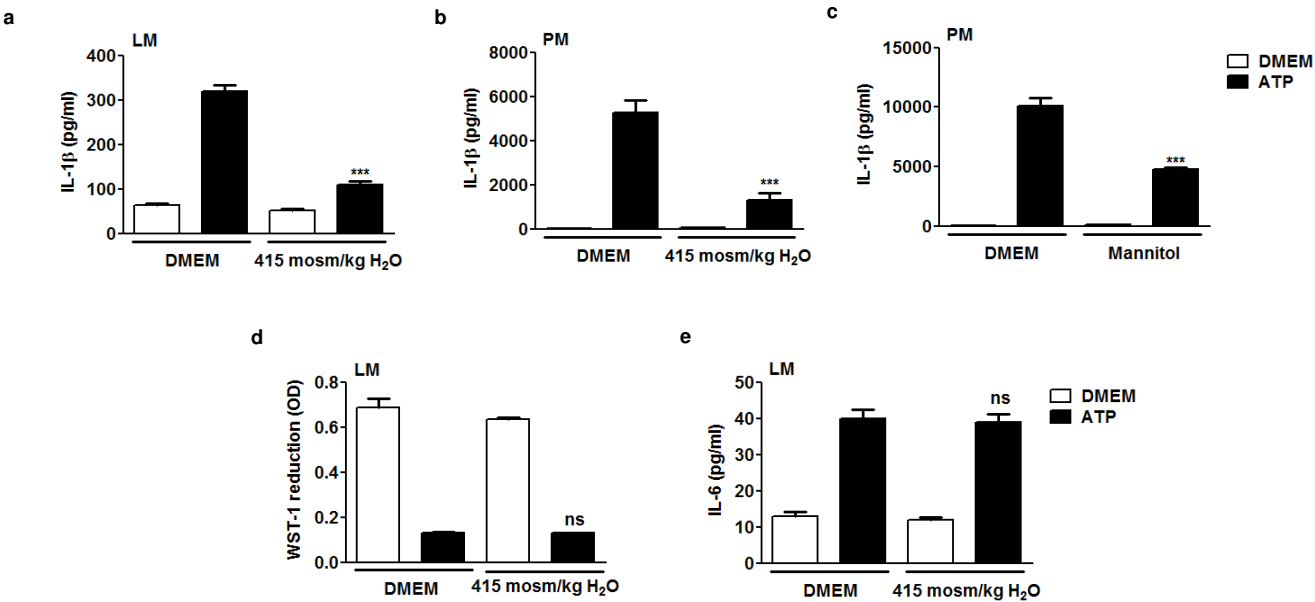
**Figure 4: AQP1 contributes to swelling, caspase-1 activation and mature IL-1 $\beta$  release in macrophages.**

(a) Flow-cytometry forward scatter plots of wild-type (WT) or AQP1 KO lung macrophages (LM) primed with LPS (0.1  $\mu$ g/ml) and subsequently subjected or not to hypotonic shock (60 mosm/kg H<sub>2</sub>O). Values indicated in plots are differences between median forward scatter of cells exposed or not to hypotonic shock. (b) IL-1 $\beta$  released by WT and AQP1 KO lung macrophages exposed or not to hypotonic medium during 1 hour. n=3 replicates per condition. (c) Western blot analysis of mature IL-1 $\beta$  (IL-1 $\beta$  p17) in the supernatant (SN) of WT and AQP1 KO lung macrophages exposed or not to hypotonic medium. (d) IL-1 $\beta$  released by WT and AQP1 KO peritoneal macrophages (PM) exposed or not to hypotonic medium (100 mosm/kg H<sub>2</sub>O) during 1 hour. n=3. (e) Fluorimetric measurement of cellular active caspase-1 in WT and AQP1 KO lung macrophages exposed or not to hypotonic medium (60 mosm/kg H<sub>2</sub>O) during 1 hour. n=3. (f) IL-1 $\beta$  release by WT and AQP1 KO lung macrophages primed with LPS (0.1  $\mu$ g/ml) and subsequently exposed or not to ATP (5 mM). n=3 or 4. (g) Western blot analysis of IL-1 $\beta$  (IL-1 $\beta$  p17) and active caspase-1 (Casp1 p10) in the supernatant of WT and AQP1 KO lung macrophages exposed or not to ATP. Mature IL-1 $\beta$  release by WT and AQP1 KO lung macrophages primed with LPS (0.1  $\mu$ g/ml) and subsequently exposed or not to (h) nigericin (ng, 20  $\mu$ M), (i) silica (DQ12, 400  $\mu$ g/ml) or (j) silica nanoparticles (SNP, 100  $\mu$ g/ml). n=3 or 4. (k) Western blot analysis of intracellular pro-IL-1 $\beta$  (IL-1 $\beta$  p37), pro-caspase-1 (Casp1 p45) and  $\beta$ -actin in LPS-primed WT and AQP1 deficient lung macrophages. (l) Intracellular levels of pro-IL-1 $\beta$  in WT and AQP1 KO lung macrophages, quantified by ELISA. n=3 or 4. Expression of (m) NLRP3 and (n) ASC transcripts quantified by qRT-PCR in WT and AQP1 KO lung. n=3 or 4. Values are means  $\pm$  SEM. \*\*\* $p < 0.001$  denote significant difference in values measured in WT or AQP1 KO cells; ns, denotes no significant difference. P-values were calculated by the Student Newman–Keuls test.

***Figure 5: Acute lung inflammatory response to silica particles is reduced in AQP1 deficient mice.***

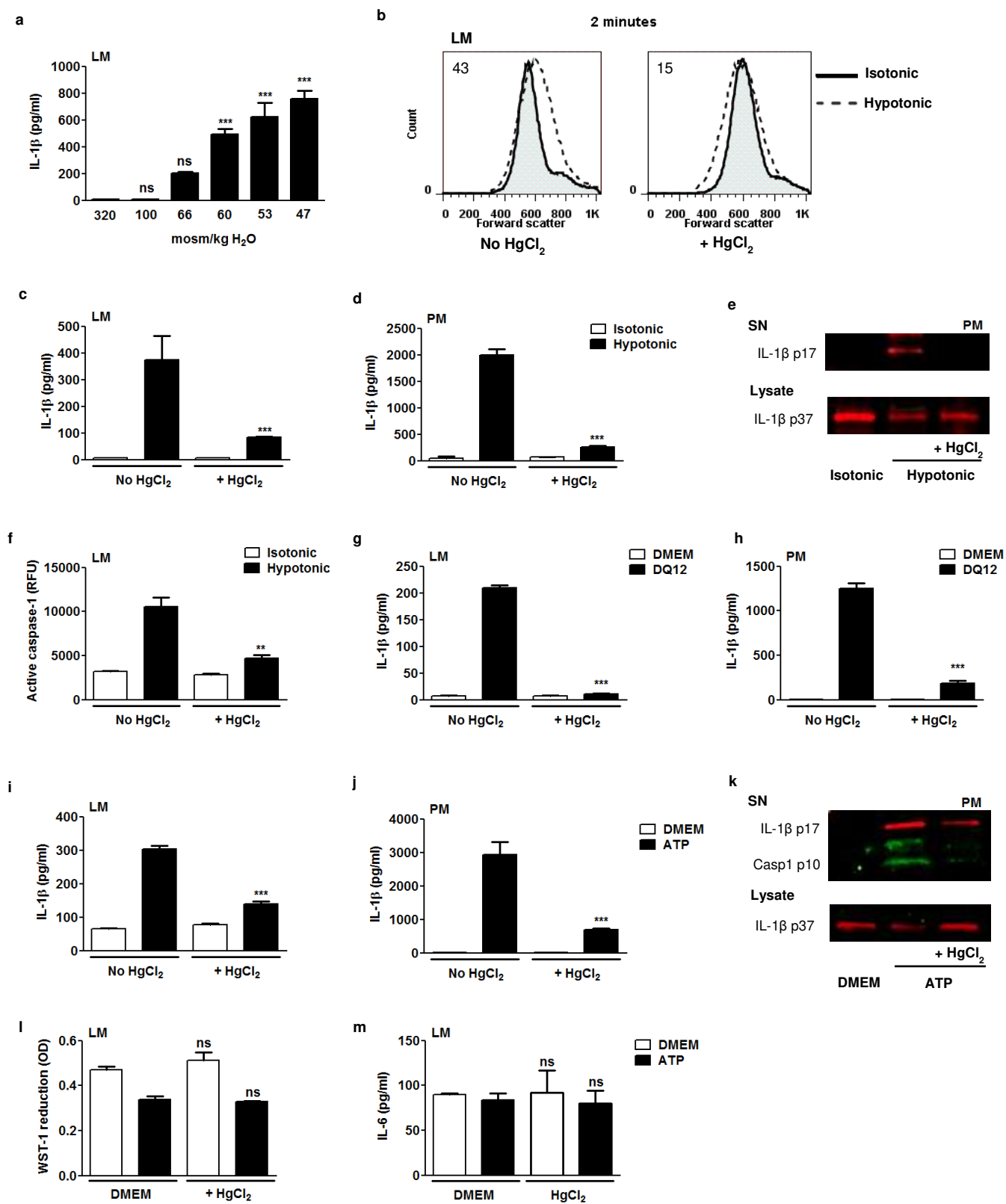
**(a)** Number of alveolar neutrophils (GR1<sup>+</sup> cells) assessed by flow cytometry and expression of pulmonary neutrophilic markers **(b)** ngp and **(c)** CXCR2 quantified by qRT-PCR in WT and AQP1 KO mice 6 hours after instillation of silica (DQ12, 2.5 mg) or not (control). **(d)** Levels of mature IL-1 $\beta$  in BAL fluid collected 6 hours after instillation of silica or not. Values are means  $\pm$  SEM; n = 3 to 6 animals per condition. **(e-h)** Hematoxylin and eosin-stained lung sections obtained from WT (e and g) or AQP1 KO mice (f and h), collected 6 hours after instillation of silica (g and h) or not (e and f). Black arrows identify neutrophils and red arrows identify silica deposition. Bars correspond to 50  $\mu$ m in large panels and to 20  $\mu$ m in the inserts. \*p<0.05, \*\*p<0.01 and \*\*\*p<0.001 denote significant difference in values measured in silica-treated WT and AQP1 KO mice. P-values were calculated by the Student Newman–Keuls test.

Figure 1





**Figure 2**



**Figure 3**

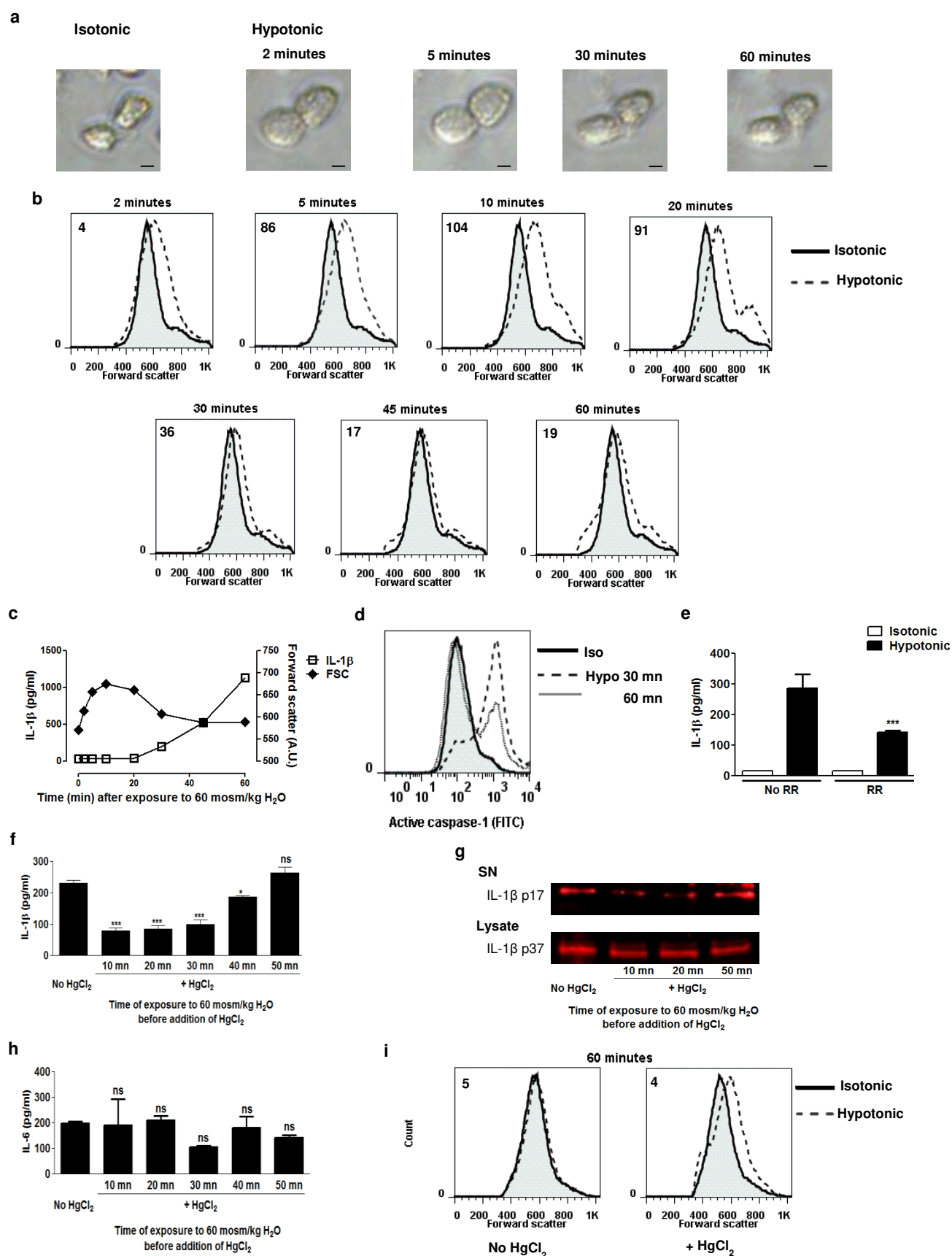


**Figure 4**

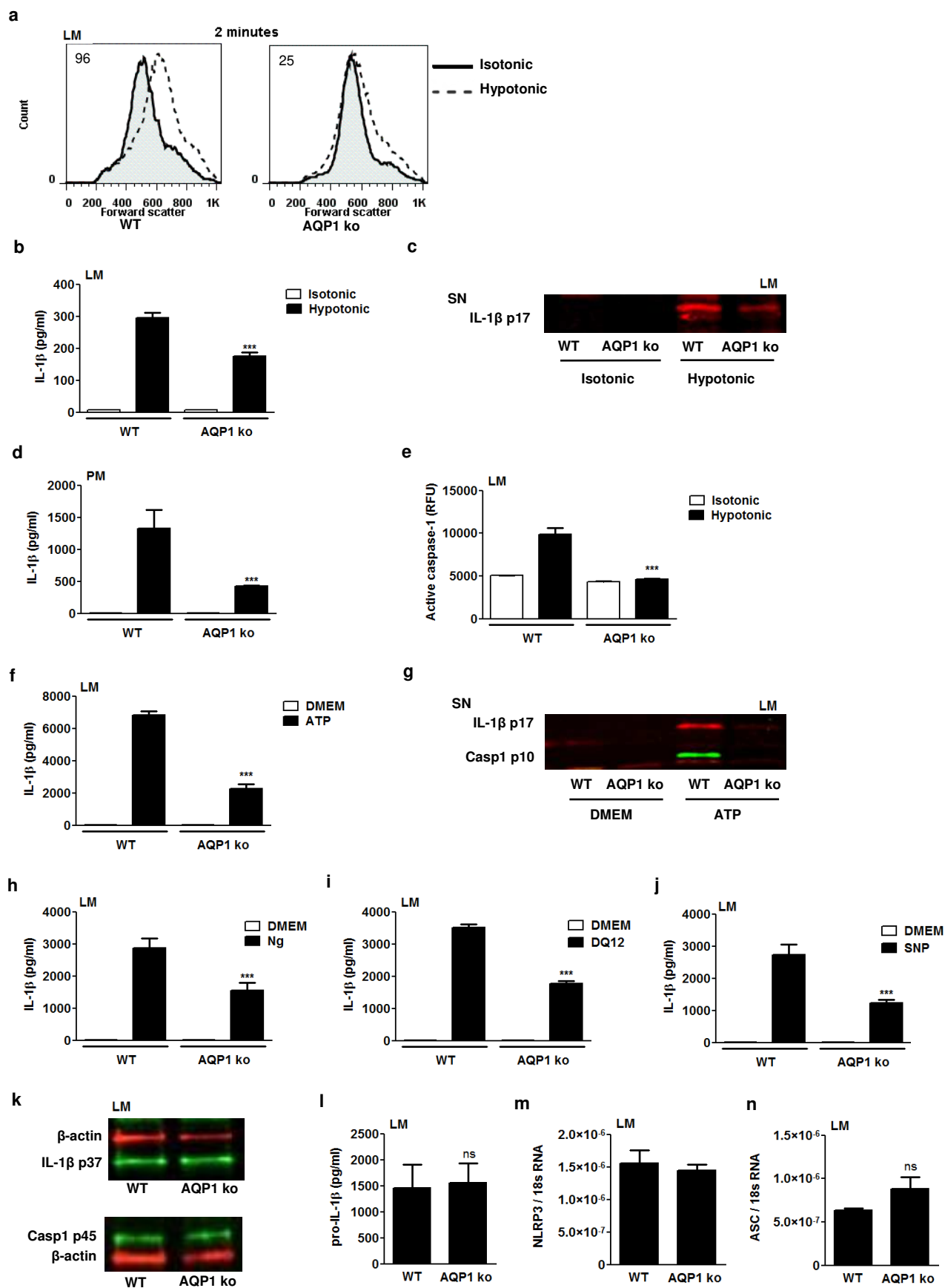
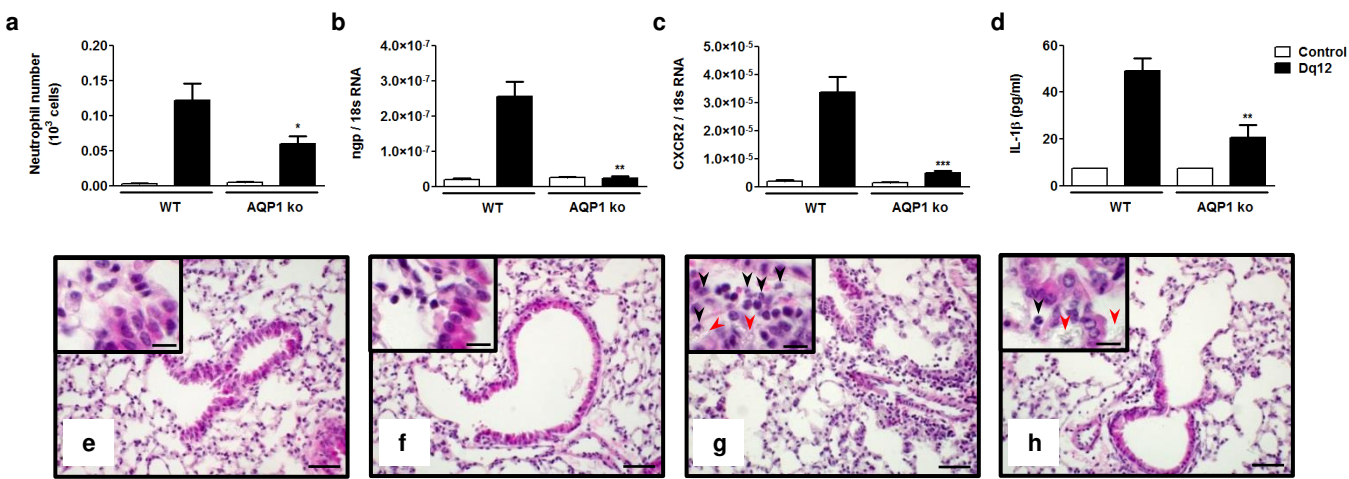


Figure 5





**Immunology:**  
**Critical role of aquaporins in IL-1 $\beta$   
-mediated inflammation.**

Virginie Rabolli, Laurent Wallemme, Sandra  
Lo Re, Francine Uwambayinema, Mihaly  
Palmai-Pallag, Leen Thomassen, Donatienne  
Tyteca, Jean-Noel Octave, Etienne Marbaix,  
Dominique Lison, Olivier Devuyst and  
François Huaux  
*J. Biol. Chem.* published online April 3, 2014



Access the most updated version of this article at doi: [10.1074/jbc.M113.534594](https://doi.org/10.1074/jbc.M113.534594)

Find articles, minireviews, Reflections and Classics on similar topics on the [JBC Affinity Sites](#).

Alerts:

- [When this article is cited](#)
- [When a correction for this article is posted](#)

[Click here](#) to choose from all of JBC's e-mail alerts

This article cites 0 references, 0 of which can be accessed free at  
<http://www.jbc.org/content/early/2014/04/03/jbc.M113.534594.full.html#ref-list-1>